Supplementary Material (ESI) for Chemical Communications

Supporting Information for:

Elaboration and properties of hierarchically structured optical thin films of MIL-101(Cr)

Aude Demessence, Patricia Horcajada, Christian Serre, Cédric Boissière, David Grosso, Clément Sanchez and Gérard Férey

Institut Lavoisier, UMR CNRS 8180, Université de Versailles, St Quentin-en-Yvelines, France. Laboratoire de Chimie de la Matière Condensée de Paris, UMR CNRS 7574, Collège de France, Université Paris 6, France.

Water was distilled and deionized prior to use. All other reagents were obtained from commercial vendors, and were used without further purification.

Synthesis of the nanoparticles of MIL101(Cr). The chromium terephthalate MIL-101 was synthesized at 200 °C for 1 min under microwave irradiation at 800 W. The molar composition of the reactant mixture was 1 $Cr(NO_3)_3 \cdot 9H_2O$: 1 H_2BDC (benzene dicarboxylate) : 300 H_2O. The reactant mixture was loaded into a Teflon autoclave, sealed, and placed in a microwave oven (Mars-5, CEM). The autoclave was heated to 200 °C in 4 min, kept at this temperature for 1 min and then carefully opened to decrease the pressure and temperature in order to stop the reaction. To remove the free acid, MIL101(Cr) nanoparticles were first filtered. Then the filtrate was centrifuged to remove the excess of $Cr(NO_3)_3$ and three cycles of redispersion in absolute EtOH / centrifugation were carried out. For analyses, the particles were dried under vacuum and for the elaboration of thin films, the particles were left in absolute EtOH.

Dried nanoparticles of MIL101(Cr) were characterized by FTIR spectroscopy. The IR spectra clearly shows vibrational bands of the –(O-C-O-) groups around 1580 and 1450 cm^{-1}, confirming the presence of the dicarboxylate functions and the absence of free acid. IR (cm^{-1}): 3400, 1625, 1584, 1447, 1385, 1144, 1110, 1090, 940, 760, 718, 668, 626, 482, 462.

Films elaboration. Thin films were prepared by dip-coating colloidal solution at room temperature and under ambient atmospheric conditions, using side polished silicon wafers as substrates and withdrawal speed of 8 $mm.s^{-1}$. The film was then maintained 2 additional min under ambient conditions before been heated at 130 °C for 5 min in air, washed with ethanol and dried at 130°C in air, which did not change the final structure. Increasing the film thickness was achieved through multiple deposition process using the same conditions. Measurement of contact angle with water was found to be around 50 °.

Experimental conditions.

The XRPD patterns were collected in a conventional high resolution (θ-2θ) D5000 Siemens X´Pert MDP diffractometer (λ_{Cu} $K\alpha_1$,.$K\alpha_2$) from 2 to 30 º (2θ) using a step of 0.02º and 30 s per step in continuous mode. Infra-red spectra were collected with a Nicolet Nexus spectrometer.

Transmission electron microscopy (TEM) was carried out using a 300 keV Philips CM30 microscope. TEM micrographs were processed with a slow scan CCD camera and analyzed with the Digital Micrograph program. Samples were prepared by adding one drop of the colloidal solution on an electronic microscope grid.

The TGA profile was obtained on a thermo-gravimetric analyzer (Model Perkin Elmer STA 6000) in air at a constant rate of 2 °C.min^{-1}.

The nitrogen sorption experiments were performed at 77 K on a Micromeritics ASAP 2010 sorption analyzer after activation of the sample (ca. 0.05 g) at 120 °C for 12 h under vacuum.

Diffusion light scattering experiments were performed on Malvern nanosizer (Nano ZS) at 173°.

Atomic Force microscopy (AFM) was carried out using a Veeco DI CPII microscope.

Ellipsometry measurements were carried out on a UV-visible (240-1000 nm) Variable Angle Spectroscopic Ellipsometer (VASE) from Woolam, and the data analysis was performed with the WVase 32 software. The thickness of the film is deduced from the UV-vis spectroscopic ellipsometry measurements, using the Cauchy model of optical dispersion in non-absorbing regions of the spectrum. Environmental ellipsometry porosity[1] involves the dynamic *in situ* monitoring of the refractive index in UV-Vis spectral range and the thickness of the film upon variation of the relative vapor pressure between 0 % and 100 % inside the analysis chamber.

Grazing-incidence wide-angle X-ray scattering (GI-WAXS) was recorded using an Rigaku S-MAX 3000 with simultaneous small angle X-ray scattering (SAXS) capabilities, on an image plate.

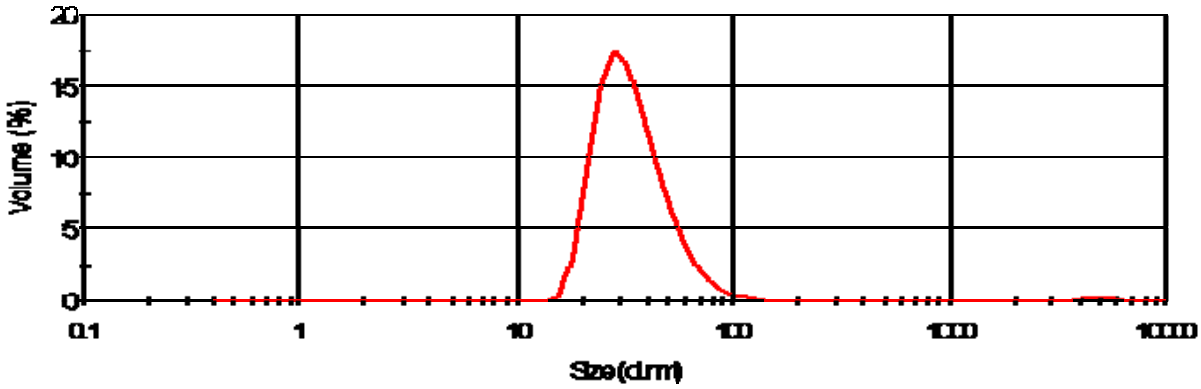

Fig. S1 Diffusion Light Scattering size distribution curve of nanoparticles of MIL101(Cr) in water at 25 °C (Z-average 49 nm, polydispersity 0.236).

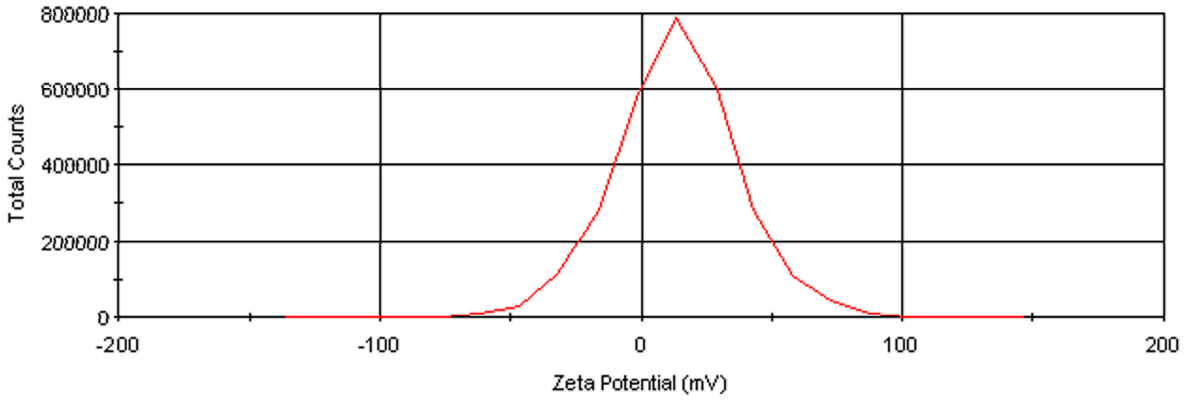

Fig. S2 Zeta potential distribution of nanoparticles of MIL101(Cr) in absolute ethanol at 25 °C (Zeta potential 13.5 mV, conductivity 0.00484 mS/cm).

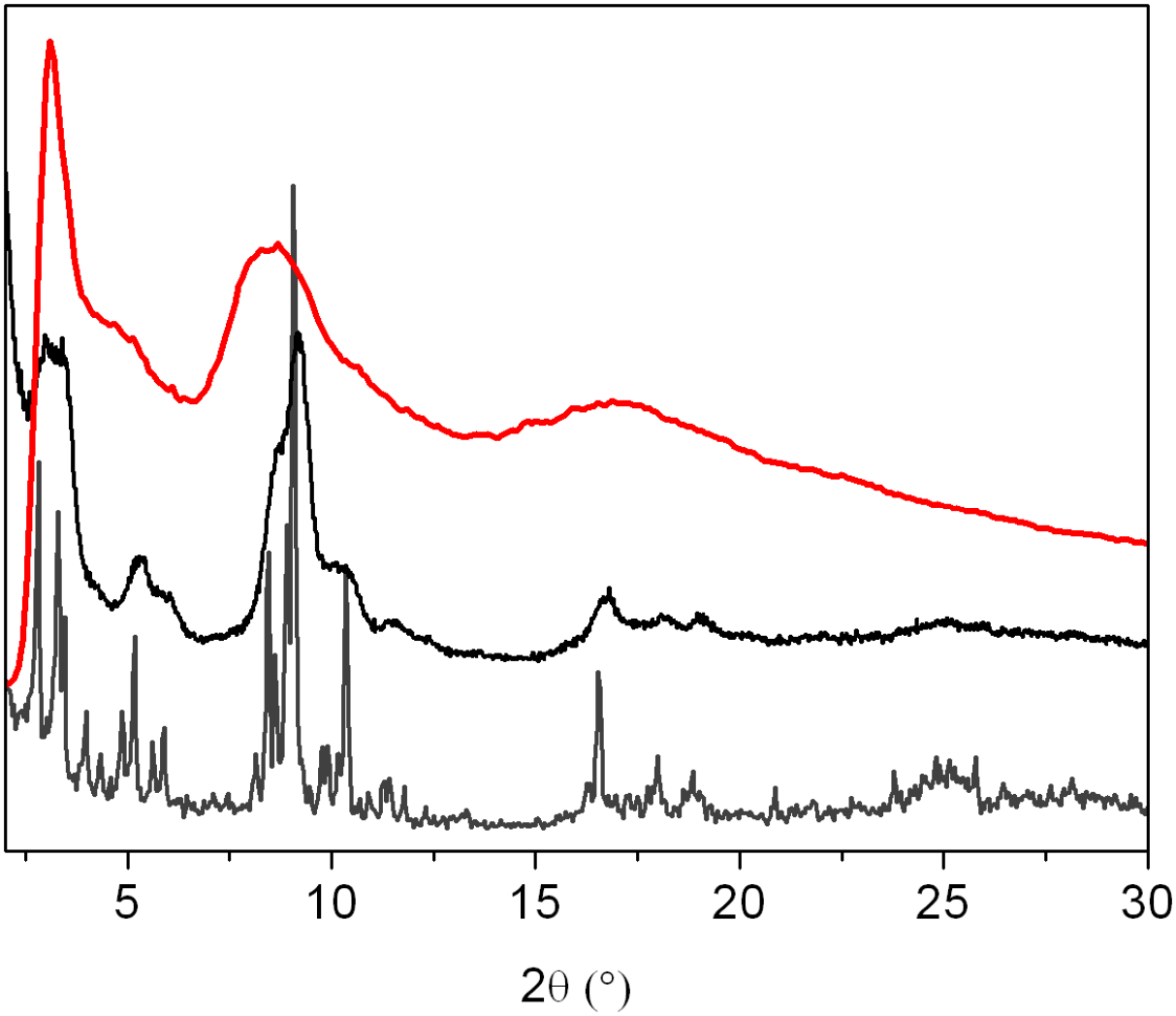

Fig. S3 XRPD pattern of bulk (grey) and nanoparticles (black), and GI-WAXS on a thin film of MIL-101(Cr) (red).

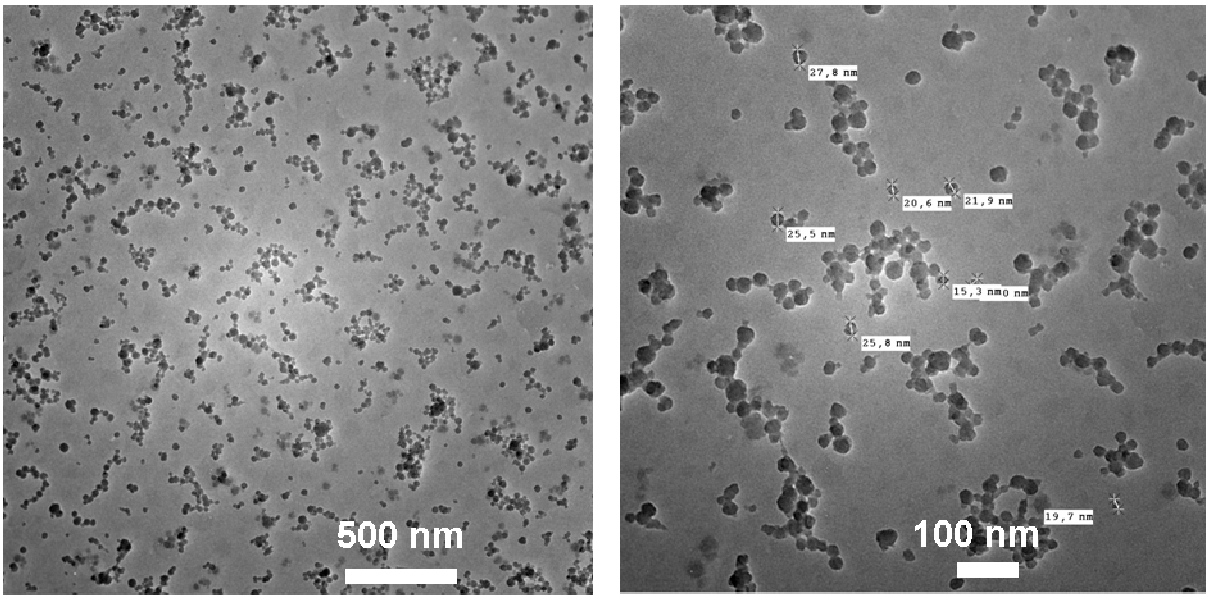

Fig. S3 TEM images of nanoparticles of MIL101(Cr).

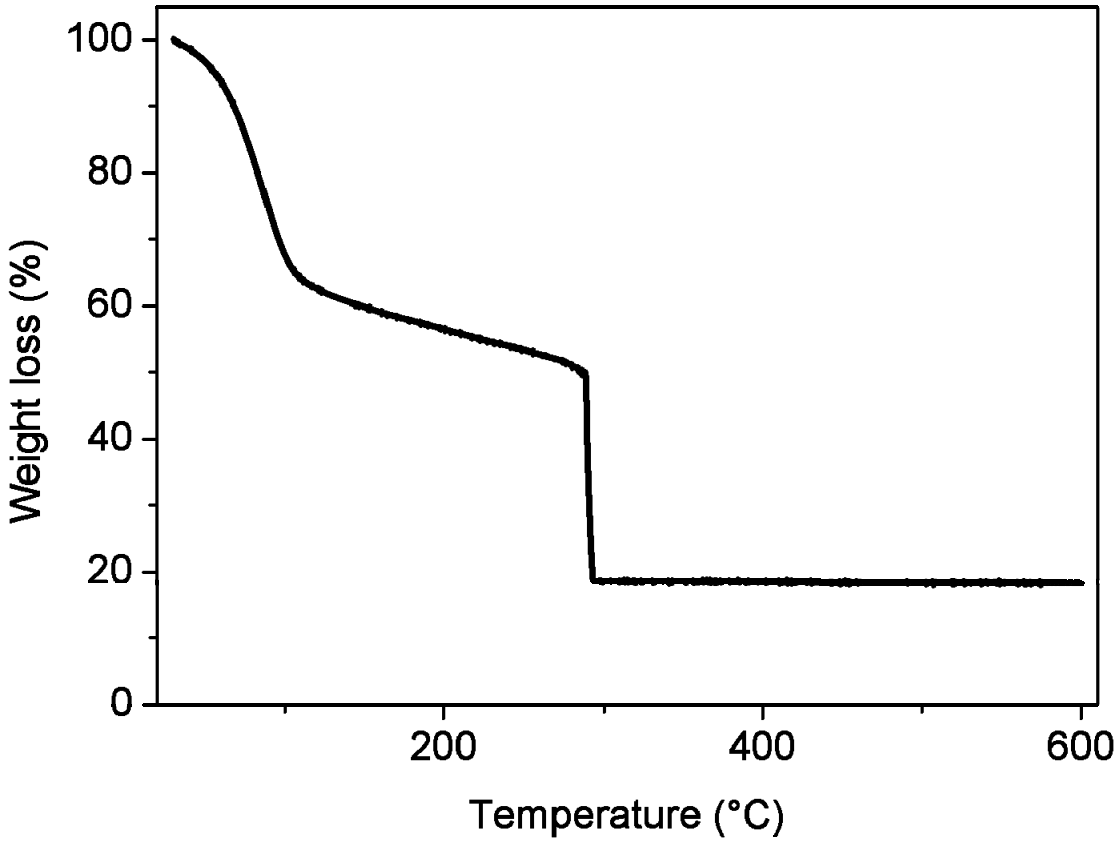

Fig. S4 TGA curve of nanoparticles of MIL101(Cr).

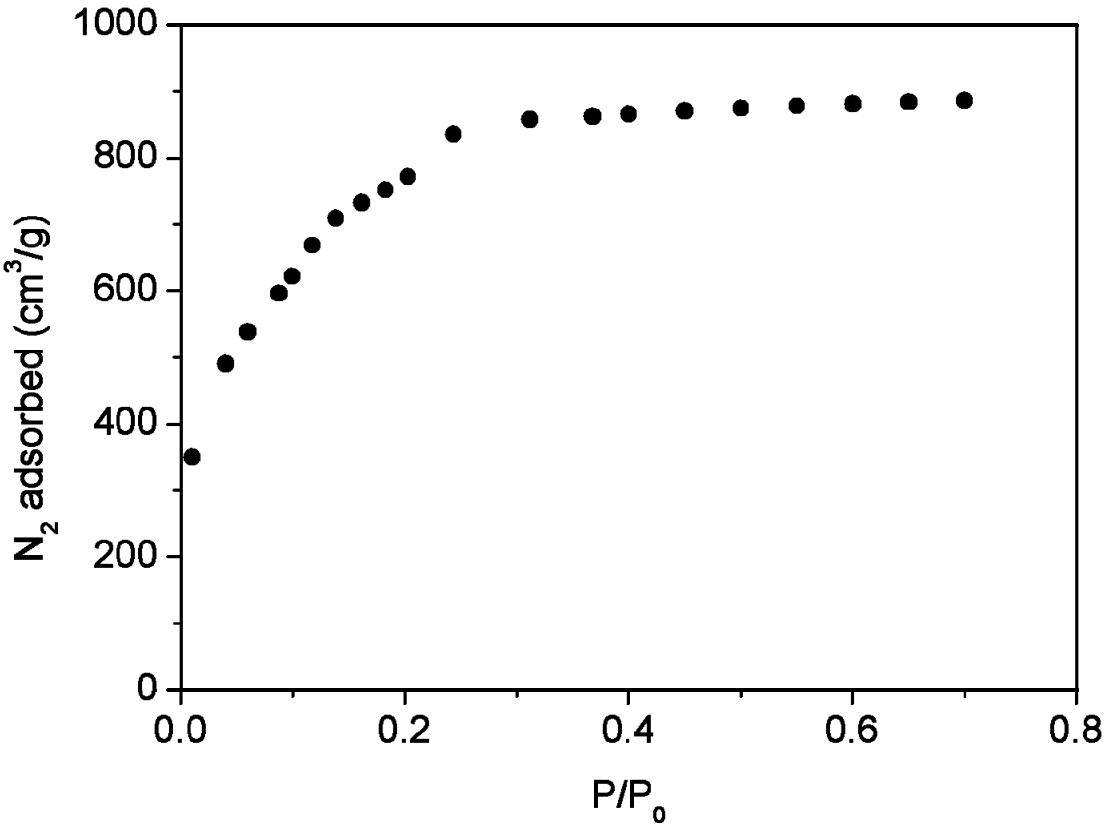

Fig. S5 N_2 adsorption isotherm at 77 K in nanoparticles of MIL101(Cr) activated at 120 °C under vacuum.

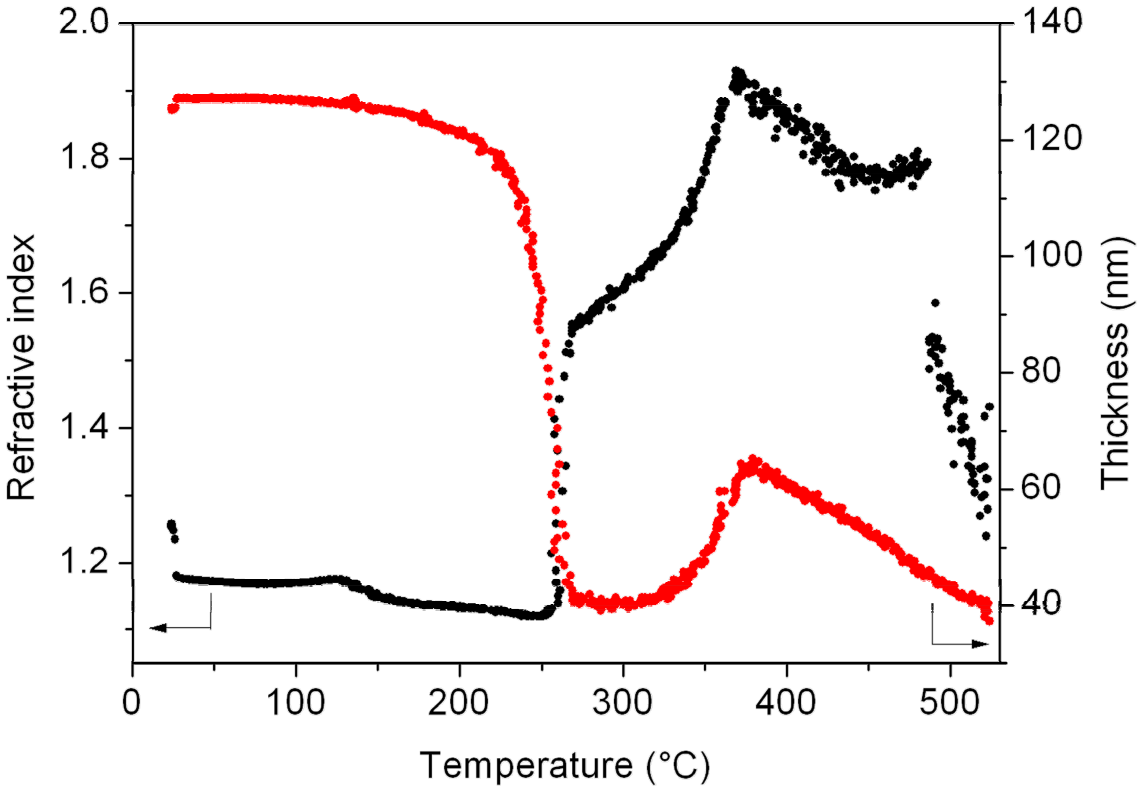

Fig. S6 Evolutions of the refractive index (black) and the thickness (red) of one-deposition MIL-101(Cr) film upon increasing temperature. Experiment carried out at 4 °C.min^{-1} under ambient atmosphere.

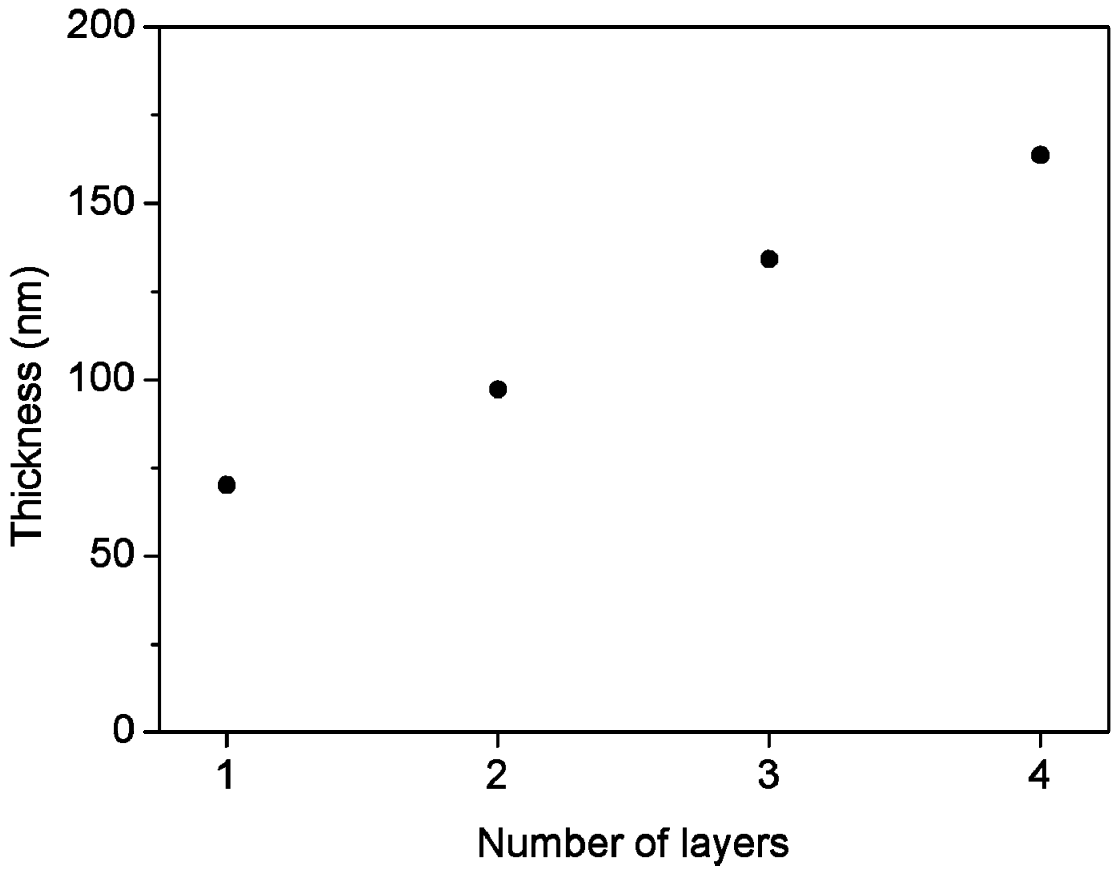

Fig. S7 Evolution of the thickness of a thin film of MIL101(Cr) with the number of depositions by dip-coating at relative humidity null (Table 1).

Table 1. Thickness and refractive index of thin films of MIL101(Cr) depending on the number of depositions by dip-coating

Number of layers	Thickness (nm)	Refractive index
1	70.0	1.117
2	97.1	1.135
3	134.1	1.134
4	163.6	1.143

Ellipsometric experiments:

Considering the refractive index of 3 cases with the empty film (or full of air) at $P/P_0 = 0$, intermediate part (MOF full of water and inter-grain full of air) at P/P_0 = and when the film is full of water at $P/P_0 = 1$ we deduced with a Cauchy model the porous volume inside the film and the refractive index at 700 nm of the dense film, 1.55 (A = 1.5138, B = 0.01722).

Table 2 Refractive indexes upon water and alcohol adsorption isotherms

	H_2O	EtOH	Isopropanol
n dense film	1.55	1.55	1.55
n empty film	1.106	1.184	1.195
n film full of vapors	1.375	1.455	1.463
Porous Vol. film (cm^3)	0.783	0.628	0.608
Porous Vol. from pores of MIL101(Cr) (cm^3)	0.23	0.25	0.23
Porous Vol. from inter-grain porosity (cm^3)	0.55	0.38	0.38

Calculs of Young's modulus (*E*) :

$E = \Delta P * d0/(d0-di)$

di: the initial film thickness

d0: the film thickness after adsorption,

ΔP, the microscopic capillary pressure across the liquid-air interface, defined by Young-Laplace equation as:

$$\Delta p = \frac{2\gamma \cos\theta}{a}.$$

cos θ is the adsorbate-film wetting angle at high partial (relative) pressure of adsorbate

γ: surface tension of adsorbate

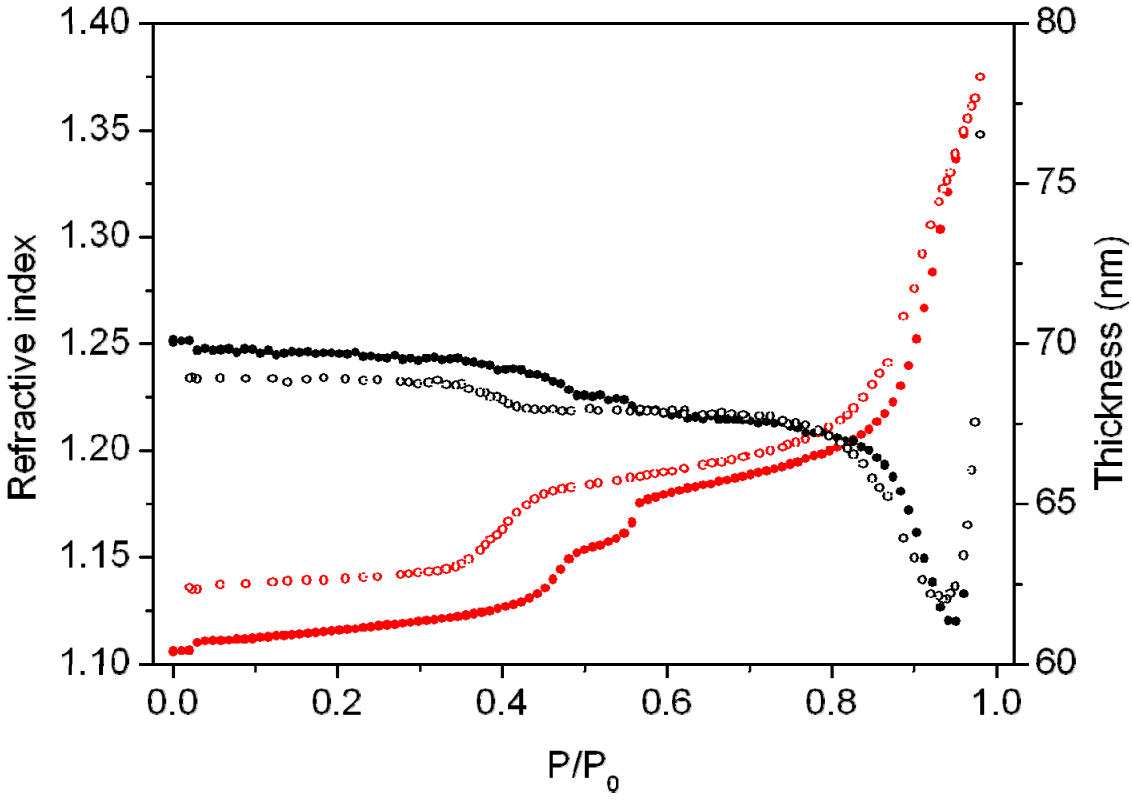

Fig. S8 Evolution of refractve index (red) and thickness (black) of one-layer of MIL-101(Cr) film as a function of relative humidity, during water adsorption (filled circles)–desorption (open circles) cycle.

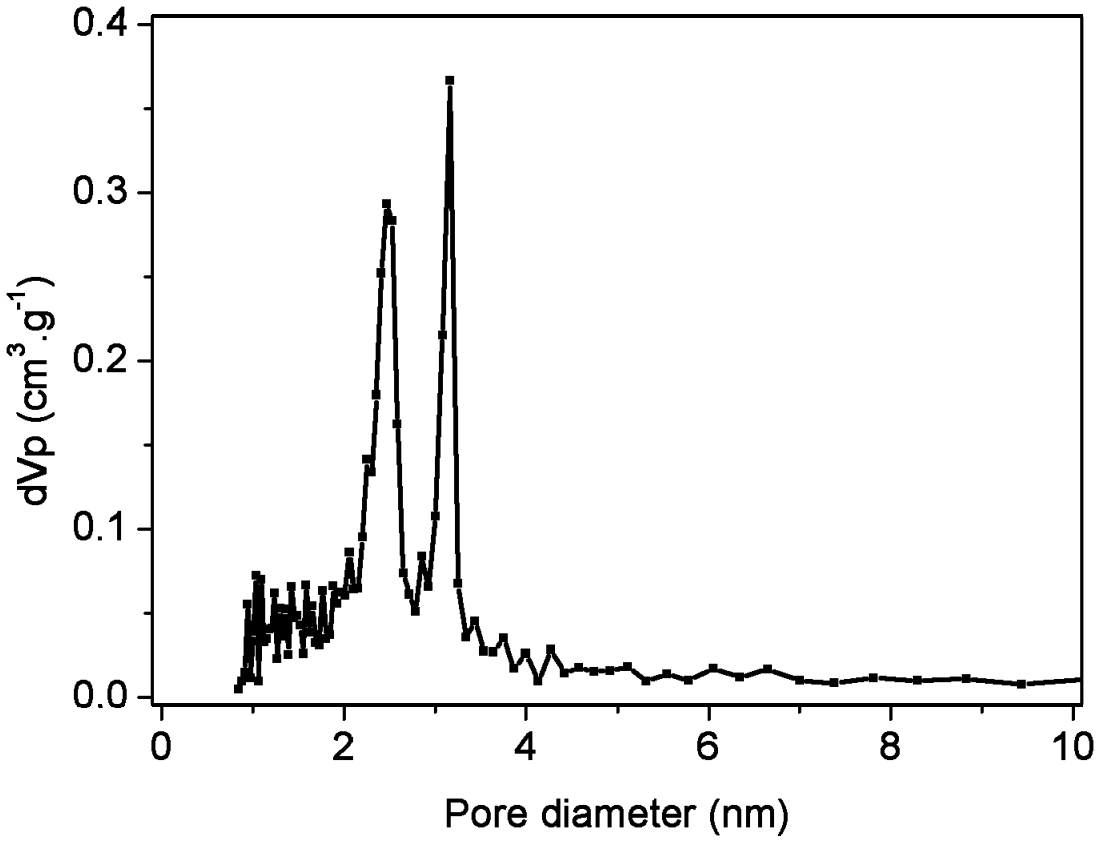

Fig. S9 Pore size distribution plot from water adsorption study at room temperature. The plot shows the existence of two maxima centred at pore radii of ca. 2.5 nm and 3.2 nm.

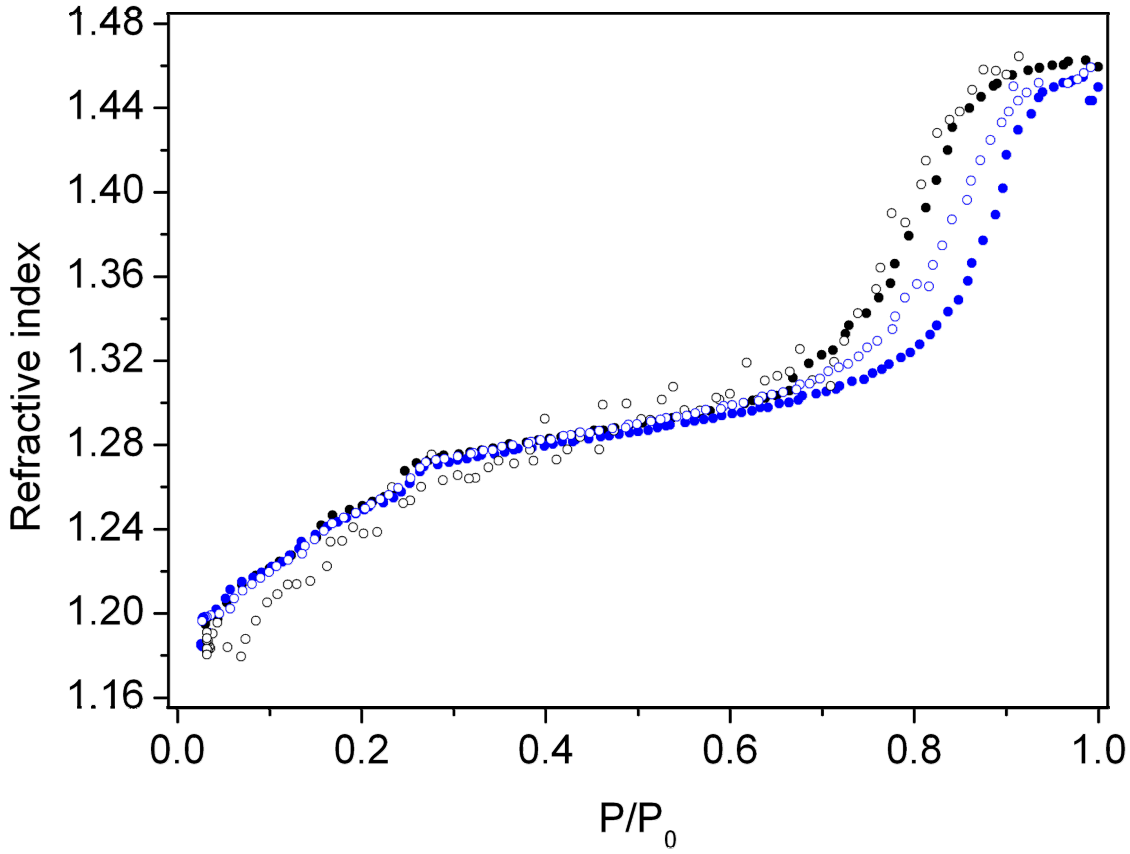

Fig. S10 Evolution of sorbed absolute ethanol (blue) and isopropanol (black) refractive index of one-deposition of MIL-101(Cr) film upon solvent adsorption (filled) – desorption (open) cycle.

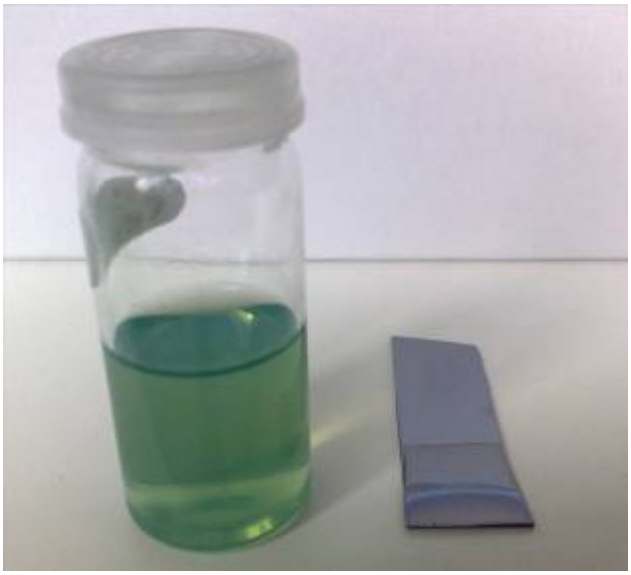

Fig. S11 Picture of the stable suspension of MIL101(Cr) nanoparticles (left) used to dip-coat high quality optical thin films on silicon wafer(right).

1. C. Boissière, D. Grosso, S. Lepoutre, L. Nicole, A. Brunet Bruneau and C. Sanchez, *Langmuir*, 2005, **21**, 12362.